

# Fluorescence Resonance Energy Transfer-Based Stoichiometry in Living Cells

Adam Hoppe,\*<sup>†</sup> Kenneth Christensen,\* and Joel A. Swanson\*<sup>†</sup>

\*Department of Microbiology and Immunology and <sup>†</sup>Biophysics Research Division, University of Michigan Medical School, Ann Arbor, Michigan 48109 USA

**ABSTRACT** Imaging of fluorescence resonance energy transfer (FRET) between fluorescently labeled molecules can measure the timing and location of intermolecular interactions inside living cells. Present microscopic methods measure FRET in arbitrary units, and cannot discriminate FRET efficiency and the fractions of donor and acceptor in complex. Here we describe a stoichiometric method that uses three microscopic fluorescence images to measure FRET efficiency, the relative concentrations of donor and acceptor, and the fractions of donor and acceptor in complex in living cells. FRET stoichiometry derives from the concept that specific donor–acceptor complexes will give rise to a characteristic FRET efficiency, which, if measured, can allow stoichiometric discrimination of interacting components. A first equation determines FRET efficiency and the fraction of acceptor molecules in complex with donor. A second equation determines the fraction of donor molecules in complex by estimating the donor fluorescence lost due to energy transfer. This eliminates the need for acceptor photo-bleaching to determine total donor concentrations and allows for repeated measurements from the same cell. A third equation obtains the ratio of total acceptor to total donor molecules. The theory and method were confirmed by microscopic measurements of fluorescence from cyan fluorescent protein (CFP), citrine, and linked CFP–Citrine fusion protein, in solutions and inside cells. Together, the methods derived from these equations allow sensitive, rapid, and repeatable detection of donor-, acceptor-, and donor–acceptor complex stoichiometry at each pixel in an image. By accurately imaging molecular interactions, FRET stoichiometry opens new areas for quantitative study of intracellular molecular networks.

## INTRODUCTION

Understanding the functions of intracellular biological molecules requires quantitative study of their localization and interaction dynamics inside living cells. Fluorescence resonance energy transfer (FRET) is a process in which an excited donor fluorophore transfers energy to a lower-energy acceptor fluorophore via a short-range ( $\leq 10$  nm) dipole–dipole interaction (Lakowicz, 1999). Binding interactions between donor-labeled and acceptor-labeled proteins can bring fluorophores within the appropriate distance for FRET to occur. Application of FRET to microscopy has become an important tool for live-cell detection of molecular interactions between fluorescently labeled molecules (Sourjik and Berg, 2002; Kraynov et al., 2000; Janetopoulos et al., 2001). Yet few FRET studies quantify the stoichiometry of molecular interactions.

Live-cell FRET studies of binding events have been further aided by the development of spectral variants of green fluorescent protein (Tsien, 1998), such as cyan fluorescent protein (CFP) and yellow fluorescent protein (YFP). CFP- and YFP-labeled chimeras coexpressed in cells as FRET donor and acceptor, respectively, have allowed microscopic localization of donor–acceptor complexes relative to cellular activities (Janetopoulos et al.,

2001). Here we demonstrate that citrine (Griesbeck et al., 2001), an improved YFP, has a longer Förster distance at neutral pH than YFP and is a superior acceptor for FRET with CFP.

Most previous applications of FRET to biological systems have utilized the  $1/r^6$  distance dependence to glean information about molecular structure. For understanding the behavior of molecular networks inside living cells, however, the structural information afforded by the distance dependence is of less interest than the magnitude and dynamics of interactions between donor- and acceptor-labeled molecules.

Although current microscopic methods for detecting FRET determine where bimolecular interactions occur in a cell (Gordon et al., 1998; Xia and Liu, 2001), they are inadequate for stoichiometric measurements of binding interactions. Existing methods quantify FRET in arbitrary units and cannot determine whether a low FRET signal is due to absence of complex or to local excesses of free donor or acceptor molecules. Erickson et al. (2001) developed a more quantitative FRET method that obtains an apparent efficiency from measurements of sensitized emission. Here we extend that work by developing new theory and methods that can image the complete stoichiometry of intermolecular binding events inside living cells. The FRET microscopic methods presented here improve quantitation by directly determining concentration ratios and fractions of interacting molecules even when the fluorescent labels have overlapping excitation and emission spectra. This approach can be utilized to image quantitatively interactions between

*Submitted June 18, 2002, and accepted for publication September 3, 2002.*

Address reprint requests to Joel A. Swanson, Dept. of Microbiology and Immunology, Univ. of Michigan Medical School, Ann Arbor, MI 48109-0620. Tel.: 734-647-6339; Fax: 734-764-3562; E-mail: jswan@umich.edu.

© 2002 by the Biophysical Society

0006-3495/02/12/3652/13 \$2.00

CFP- and citrine-labeled molecules in living cells. Application of FRET stoichiometry to fluorescent chimeras that are intrinsic components of signaling pathways will allow quantitative analysis of the spatially organized chemistries that constitute signal transduction.

## MATERIALS AND METHODS

### Constructs and protein purification

pEYFP-C1 and pECFP-N1 (Clontech, Palo Alto, CA) were used directly or pEYFP-C1 was mutated (Q69M) by the Quickchange Method (Stratagene, La Jolla, CA) to produce citrine. The CFP coding region of pECFP-N1 was PCR amplified with a primer coding for an additional four glycines, restriction digested, and inserted into the pEYFP-C1 or Citrine vector between the *HindIII* and *EcoRI* restriction sites. This produced the fusions CFP-YFP and CFP-Cit, each with a 16-amino acid linker between the fluorescent proteins.

#### PCR Primers:

5'-ATGCAAGCTTCGGGAGGAGGAGGAGGCGGCATGGTGAGC-AAGGGCGAGGAG

5'-CAAGAATTCTTACTTGACAGCTCGTCCAT

The coding sequences for CFP, YFP, Citrine, CFP-YFP, and CFP-Cit were cloned into pQE-31 (Qiagen, Chatsworth, CA) prokaryotic expression vector at the *XmaI* site to add a 6-His tag at the *N*-terminus. The plasmid was transferred to JM109 *E. coli*. The cells were grown with shaking (150 RPM) at 37°C in LB, to an OD<sub>600</sub> of 0.7 and induced with isopropylthio-β-D-galactoside (PTG) for 7 h. After induction, the culture was chilled on ice 15 min, pelleted by centrifugation (5000 × *g*, 15 min) and resuspended in lysis buffer with lysozyme for 15 min. Lysates were passed through a French press, treated with DNase and RNase for 10 min at 4°C, cleared by centrifugation (15,000 × *g*, 30 min), and the proteins were purified on Ni-NTA agarose according to the manufacturer's protocol (Qiagen). SDS-PAGE stained with Coomassie Blue showed the proteins to be greater than 98% pure.

### Cell culture and transfection of J774 macrophages

J774.A1 cells obtained from ATCC were grown in Dulbecco's modified Eagle's medium supplemented with 10% fetal bovine serum (Gibco BRL, Gaithersburg, MD) (heat-inactivated at 56°C for 45 mins) and 100 unit/mL of penicillin/streptomycin mixture (Sigma, St. Louis, MO) at 37°C with 5% CO<sub>2</sub>. Macrophages were plated on acid-washed coverglasses 24 h prior to transfection. Transfection was carried out 24 h prior to the experiment with 1 μg total plasmid DNA and 2 μl FuGene6 (Roche, Indianapolis, IN). During microscopic observation, the cells were maintained at 37°C on a heated stage in Ringer's buffer.

### Image acquisition

The FRET microscope consisted of an inverted fluorescence microscope (Nikon TE-300, Melville, NJ), equipped with a temperature-controlled stage, a 75-W mercury arc lamp, shutters for trans- and epifluorescence illumination, filter wheels for both excitation and emission filters, dichroic mirrors that allowed simultaneous detection of multiple fluorophores, a 60× Planapo objective, and a cooled digital CCD camera (Quantix, Photometrics, Tucson, AZ), all of which were controlled by Metamorph image-processing software (version 4.6.2, Universal Imaging, Inc., Malvern, PA). Excitation and emission filters were selected using two filter wheels (Sutter Instrument Co., Novato, CA) and a double pass dichroic

mirror bandpass combination (436-510 DBDR and 475-550 DBEM, Omega Optical, Brattleboro, VT).  $I_A$  was obtained with 510 ± 12-nm excitation and 535 ± 13-nm emission,  $I_D$  was imaged using 436 ± 5-nm excitation and 480 ± 15-nm emission, and the  $I_F$  image was collected by exciting with the 436 ± 5-nm filter and collecting the emission with the 535 ± 13-nm filter (Omega Optical).

### Image processing

All images were collected with an exposure time of 200 ms. The images were then background-subtracted and shading-corrected using the "Correct Shade" tool in MetaMorph, which performs the shading correction as Corrected Image = (Max value of Shade Image) \* (Acquired Image - Background)/(Shade Image - Background). The background image was a 20-frame average of the camera bias, taken with the identical situation as for imaging, but with the excitation light blocked. The shade image was collected from a 20-frame average of images of purified solutions of citrine or CFP, sandwiched between two BSA-coated coverglasses supported by coverglass fragments in 1 mg/ml electrophoresis grade BSA and 15 mM HEPES, 15 mM MES, 130 mM KCl, 1 mM MgCl, pH = 7.2. Shading correction was necessary to obtain uniform values of  $E_A$ ,  $E_D$ , and  $R$  across the CCD chip.

After background and shading correction, the corrected  $I_D$  and  $I_A$  images were added and a manual threshold was applied to the ADD image (Table 1). The threshold was used to generate a single binary mask that was then taken as a logical AND with each of the corrected  $I_A$ ,  $I_D$ , and  $I_F$  images. The masked images were then used to produce the FRET stoichiometry images by image arithmetic with the equations (derived in appendix and results):

$$f_A = \gamma \left[ \frac{I_F - \beta I_D}{\alpha I_A} - 1 \right] \left( \frac{1}{E_C} \right),$$

$$f_D = \left[ 1 - \frac{I_D}{(I_F - \alpha I_A - \beta I_D)(\xi/\gamma) + I_D} \right] \left( \frac{1}{E_C} \right),$$

$$R = \left( \frac{\xi}{\gamma^2} \right) \frac{\alpha I_A}{(I_F - \alpha I_A - \beta I_D)(\xi/\gamma) + I_D}.$$

### Determination of efficiency and $E_C$ by fluorescence lifetime

Experimental measurements of  $f_A$  and  $f_D$  required measurement of the characteristic efficiency of a linked construct ( $E_C$ ), in which  $f_A$  and  $f_D$  = 1.0. Solutions of, and cells expressing, either CFP or the linked CFP-Cit construct were measured on a custom lifetime fluorometer or fluorescence lifetime microscope (with identical emission optics as the steady-state microscope) configured for time-correlated single photon counting to determine  $E_C$ . The excitation for both was a mode-locked Tsunami Ti:Sapphire laser pumped with a 532-nm Millennia V laser emitting 1-ps 872-nm pulses, pulse-picked to 8 MHz and frequency doubled in a Model 3980 frequency doubler (Spectra Physics, Mountain View, CA) to provide 436 nm picosecond pulses. Lifetime measurements of purified CFP-Cit, CFP-YFP, and CFP were carried out in the custom fluorometer (Optical Building Blocks, PTI, Lawrenceville, NJ). The optical path for the microscope was the same as the steady-state microscope described above, except the excitation filter wheel was replaced with the light from the Ti:Sapphire laser. Emission wavelengths were selected by a monochromator (fluorometer) or optical bandpass filters in the microscope emission filter wheel (as above) in front of the detector (H3809, Hamamatsu City, Japan). An instrument response function (IRF) was obtained from light scattered from a solution of glycogen placed in the fluorometer or in a custom-fabricated chamber positioned in place of the microscope cube. The fluorescence

**TABLE 1** Glossary of symbols for FRET stoichiometry

Symbols	Description
$I_A$	Intensity or image at the acceptor excitation and acceptor emission.
$I_D$	Intensity or image at the donor excitation and donor emission.
$I_F$	Intensity or image at the donor excitation and acceptor emission.
$E_A$	Efficiency calculated from sensitized emission (A denotes dependence on the fraction of acceptor in complex).
$E_D$	Efficiency calculated relative to donor fluorescence (D denotes dependence on the fraction of donor in complex).
$R$	The molar ratio of acceptor to donor measured by FRET stoichiometry.
$E_C$	Characteristic FRET efficiency. Measure of the FRET efficiency for a particular molecular interaction.
$f_A$	Fraction of acceptor in complex as measured by FRET stoichiometry.
$f_D$	Fraction of donor in complex as measured by FRET stoichiometry.
$\alpha$	Proportionality constant relating acceptor fluorescence at the acceptor excitation to the donor excitation.
$\beta$	Proportionality constant relating donor fluorescence detected at the acceptor emission relative to that detected at the donor emission.
$\gamma$	Ratio of the extinction coefficient of the acceptor to the donor at the donor excitation.
$\xi$	Proportionality constant relating the sensitized acceptor emission to the decrease in donor fluorescence due to FRET.

decays were collected with a TimeHarp photon-counting computer card and analyzed with the software FluoFit 3.0 (both from PicoQuant GmbH, Berlin-Adlershof, Germany). The CFP lifetime was well fit by a double exponential in the absence of energy transfer and by a triple exponential in the presence of energy transfer. All mean lifetimes were calculated by fitting the CFP lifetime to a triple exponential. From these measurements of the mean fluorescence lifetime of CFP and of CFP–Cit,  $E_C$  of CFP–Cit was determined to be 0.40 in solutions (pH = 7.2) and 0.37 inside cells according to

$$E = \left[ 1 - \frac{\tau_{DA}}{\tau_D} \right],$$

where  $\tau_D$  and  $\tau_{DA}$  are the mean fluorescence lifetime of CFP alone or CFP–Cit, respectively. For the pH titrations, the same procedure was applied to ~1  $\mu$ M purified CFP, CFP–YFP, and CFP–Cit in 1 mg/ml BSA, 15 mM HEPES, 15 mM MES, 130 mM KCl, 1 mM MgCl<sub>2</sub>, at the pHs indicated in Fig. 3.

### Determination of the parameters $\alpha$ , $\beta$ , $\gamma$ , $\xi$

The parameters  $\alpha$  and  $\beta$ , defined previously by others (Erickson et al., 2001; Gordon et al., 1998; Xia and Liu, 2001; Youvan et al., 1997), were measured in cells transfected with DNA encoding either citrine or CFP. The images  $I_A$ ,  $I_D$ , and  $I_F$  were collected from ~25 cells for each condition.  $\alpha$  and  $\beta$  were calculated from the shading-corrected images of cells expressing only citrine ( $\alpha$ ) or CFP ( $\beta$ ) as

$$\alpha = \frac{I_F}{I_A}, \quad \beta = \frac{I_F}{I_D}.$$

$\alpha$  and  $\beta$  for our system were 0.29 and 1.07, respectively. These values were also obtained from measurements of solutions of purified citrine and CFP, and were found to be in good agreement with the cellular measurements.

Once  $\alpha$  and  $\beta$  were known,  $\gamma$  and  $\xi$  were determined by back-calculating from the equations for  $f_A$  and  $f_D$  in which  $I_A$ ,  $I_D$ , and  $I_F$  were collected from ~25 cells expressing CFP–Cit.

$$\gamma = \frac{E_C}{\left[ \frac{I_F - \beta I_D}{\alpha I_A} - 1 \right]}, \quad \xi = \frac{\gamma I_D E_C}{(1 - E_C)(I_F - \alpha I_A - \beta I_D)}$$

$\gamma$  and  $\xi$  were determined to be 0.080 and 0.012 for our system.

### Modeling

Currently, there are four published methods for detection of FRET from steady-state images of interacting molecules. These are  $N_{\text{FRET}}$  (Xia and Liu, 2001), FRETN (Gordon et al., 1998), FR (Erickson et al., 2001) and the FRET ratio ( $I_F/I_D$ ) (Miyawaki et al., 1997). FRETN has been shown to be intensity dependent and is consequently a misleading indicator of FRET (Xia and Liu, 2001). FR is equivalent to the expression of  $E_A$  presented in this manuscript.  $N_{\text{FRET}}$  is expressed in the nomenclature of this paper as

$$N_{\text{FRET}} = \frac{I_F - \alpha I_A - \beta I_D}{\sqrt{I_A \times I_D}}.$$

To evaluate the behavior of FRET stoichiometry against physical constraints and other methods such as  $N_{\text{FRET}}$  and the ratio of  $I_F/I_D$ , we generated a static model in which total donor and acceptor were assigned a concentration. The concentration of donor–acceptor complexes was then set by changing the fraction of donor or acceptor in complex. The fluorescence detected from donor or acceptor, for a given set of excitation and emission bandpasses, were related to the concentration by proportionality constants  $P_1$  and  $P_2$ , respectively. The interrelationships between filters and fluorescence excitation and emissions were set by parameters measured from our microscope system  $\alpha = 0.29$ ,  $\beta = 1.07$ ,  $\gamma = 0.08$ ,  $\xi = 0.022$  (this value for  $\xi$  was estimated before experimental measurement, the measured value was 0.012). For example, the fluorescence intensity in  $I_D$  is equal to the concentration of total donors  $[D_T]$  times a proportionality constant  $P_1$  less the fraction energy ( $E$ ) not emitted from the fraction of donor molecules ( $f_D$ ) in complex

$$I_D = P_1[D_T](1 - f_DE).$$

The acceptor fluorescence in  $I_A$  is unaffected by FRET and is proportional ( $P_2$ ) to the concentration of total acceptors  $[A_T]$  present,

$$I_A = P_2[A_T].$$

$I_F$  is made up of a portion of the donor spectrum, related to  $I_D$  by  $\beta$ , plus the portion of emissions from the acceptor whose fluorescence is related to  $I_A$  by  $\alpha$ . The acceptor emission is made up of direct excitation plus the sensitized emission from the fraction of energy transferred ( $E$ ) to the fraction of acceptors in complex ( $f_A$ ).  $\gamma$  normalizes the quantity of energy absorbed by the donor and transferred to the acceptor to the fraction of energy absorbed by direct excitation of the acceptor. For simplicity, the model is presented as though the quantum yield of the acceptor is unity; however, this was not required. In the case given here, the parameter  $\xi$  simply relates the portion of wavelengths detected from the emission

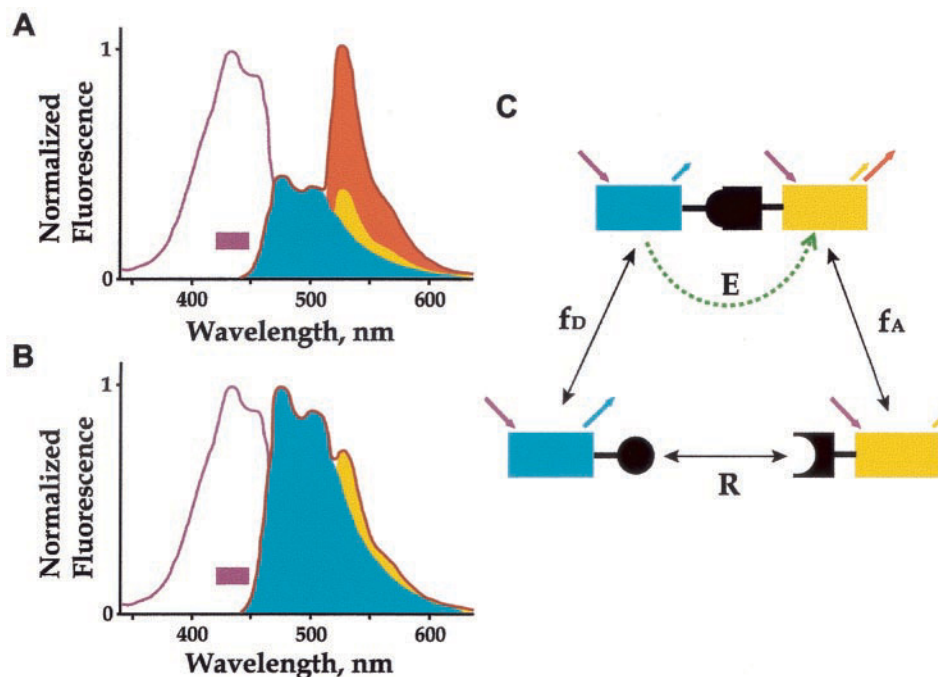


FIGURE 1 The concept of FRET stoichiometry. Component signals of emission spectra for mixtures of CFP (donor) and YFP or Citrine (acceptor) with (A) and without (B) FRET. The region of the CFP excitation spectrum (violet line) transmitted by the donor excitation filter (violet rectangle) excites CFP and, to a lesser extent, YFP. Consequently, the emission spectra (red line) contain component signals from both fluorophores. For molecules in complex that undergo FRET (A), donor fluorescence (cyan) decreases, stimulated acceptor emission due to FRET (salmon) increases, and non-FRET acceptor fluorescence (yellow) remains unchanged, relative to molecules not in complex (B). (C) Interactions between donor, acceptor, and donor-acceptor complexes influence the emission spectrum through four parameters: the efficiency of energy transfer ( $E$ ) of donor-acceptor complexes, the fraction of acceptor molecules in complex ( $f_A$ ), the fraction of donor molecules in complex ( $f_D$ ), and the ratio of total acceptor to total donor ( $R$ ). Arrows indicate fluorescence excitation (violet) and component donor fluorescence (cyan), non-FRET acceptor fluorescence (yellow), and stimulated acceptor emission by FRET (salmon).

spectrum of the donor to the acceptor and is determined by the ratio of  $P_1$  and  $P_2$ ,

$$I_F = \alpha P_2 \left[ \frac{f_A E}{\gamma} + 1 \right] [A_T] + \beta P_1 [D_T] (1 - f_D E).$$

## RESULTS

FRET stoichiometry used the same measurements as previously described by others (Youvan et al., 1997; Gordon et al., 1998; Xia and Liu, 2001; Erickson et al., 2001). Images for microscopic detection of FRET were obtained using three combinations of excitation and emission filters: donor excitation plus donor emission, acceptor excitation plus acceptor emission, and donor excitation plus acceptor emission, producing the corresponding fluorescence intensities  $I_D$ ,  $I_A$ , and  $I_F$ .  $I_D$  and  $I_A$  discriminated donor and acceptor fluorescence with negligible excitation or emission of one fluorophore in the other's filter combination.

In steady-state measurements, FRET manifests itself as a loss of fluorescence from the donor and an increase in fluorescence from the acceptor. Thus for a fixed concentration of molecules, FRET results in an increase in  $I_F$ , a

decrease in  $I_D$  and no change in  $I_A$  (Fig. 1, A and B). This simple relationship is complicated by the overlapping excitation and emission spectra of most fluorophores, including the fluorescent proteins.  $I_F$  often contains signal due to spectral overlap of the donor and acceptor emissions, even for mixtures of uncomplexed donor and acceptor that do not exhibit FRET. Under experimental conditions, the concentrations of donor and acceptor vary widely between and within cells due to differences in localization and expression levels. This means that the intensities  $I_D$ ,  $I_A$ , and  $I_F$  depend on the relative concentrations of donors, acceptors, and interacting molecules (stoichiometry) and the efficiency at which energy is transferred from the donor to the acceptor (FRET efficiency) (Fig. 1 C). Fortunately, information about stoichiometry and efficiency is contained in the three images (Fig. 1, A–C).

FRET stoichiometry measures FRET efficiencies and the fractions of donor- and acceptor-labeled molecules in complex for donor-acceptor pairs where non-FRET acceptor fluorescence is detectable in  $I_F$ . For a bimolecular interaction, the efficiency of energy transfer is calculated from



sensitized acceptor emission (Lakowicz, 1999) for molecules with overlapping spectra as (derivation in Appendix)

$$E = \gamma \left[ \frac{I_F - \beta I_D}{\alpha I_A} - 1 \right] \left( \frac{1}{f_A} \right), \quad (1)$$

where  $E$  is the FRET efficiency of the donor–acceptor complex,  $f_A$  is the fraction of acceptor in complex with donor,  $\alpha$  and  $\beta$  are independently measured proportionality constants for acceptor and donor fluorescence, respectively (i.e.,  $\alpha = I_F/I_A$  when only acceptor is present, and  $\beta = I_F/I_D$  when only donor is present), and  $\gamma$  is the ratio of the extinction coefficients of the acceptor to the donor over the donor's excitation wavelengths (Lakowicz, 1999; Erickson et al., 2001).

### The fraction of acceptor in complex ( $f_A$ )

For cellular measurements, the fraction of acceptor in complex is generally not known. Because energy transfer is dependent on both the distance and orientation of the transition dipole moments between the two fluorophores, molecular interactions for a specific pair of donor and acceptor molecules will result a characteristic FRET efficiency ( $E_C$ ) for that interaction. This can be thought of as a distance and orientation distribution induced by a particular molecular binding event for which  $E_C$  describes the mean of the distribution. If  $E_C$  for a given donor–acceptor pair can be determined from independent measurements, then the fraction of acceptor-labeled molecules in complex ( $f_A$ ) can be obtained,

$$f_A = \frac{[C]}{[A_T]} = \gamma \left[ \frac{I_F - \beta I_D}{\alpha I_A} - 1 \right] \left( \frac{1}{E_C} \right), \quad (2)$$

where  $[C]$  is the concentration of donor–acceptor complex, and  $[A_T]$  is the total concentration of acceptor (free plus complexed). If  $E_C$  is not known, or if the interaction involves multiple acceptors, then an apparent efficiency ( $E_A$ ) can be measured, which is the product of the true efficiency and the fraction of acceptor in complex (this is equivalent to  $E_{EFF}$  from Erickson et al. 2001),

$$E_A = E f_A = \gamma \left[ \frac{I_F - \beta I_D}{\alpha I_A} - 1 \right]. \quad (3)$$

Importantly,  $E_A$  is still proportional to the fraction of acceptor in complex and can be used to measure changes in the fraction of molecules in complex.

### The fraction of donor in complex ( $f_D$ )

The fraction of donor in complex ( $f_D$ ) can also be obtained from  $I_D$ ,  $I_A$ , and  $I_F$  by estimation of donor fluorescence in the absence of FRET. Others have determined this by measuring the increase in donor fluorescence after photobleach-

ing the acceptor (Kenworthy et al., 2000; Zacharias et al., 2002), but this method is slow and does not allow for repeated measurements of the same cell. Instead, the donor fluorescence lost due to FRET can be estimated by independently calibrating the extent to which stimulated acceptor emission increases as donor fluorescence decreases (Tron et al., 1984; Gordon et al., 1998). Accordingly, total donor fluorescence can be measured as  $I_D$  plus the corrected sensitized acceptor emission, then used to calculate the fraction of donor in complex,

$$f_D = \frac{[C]}{[D_T]} = \left[ 1 - \frac{I_D}{(I_F - \alpha I_A - \beta I_D)(\xi/\gamma) + I_D} \right] \left( \frac{1}{E_C} \right), \quad (4)$$

where  $[C]$  and  $[D_T]$  are the concentration of complex and total donor, respectively, and  $\xi$  relates the quantity of sensitized emission (*salmon* in Fig. 1 *A*) detected in  $I_F$  relative to the donor fluorescence (cyan in Fig. 1 *A*). That is,  $\xi$  accounts for the fraction of sensitized acceptor emission detected in  $I_F$  relative to the fraction of donor fluorescence lost by FRET. For fluorescent protein acceptors such as citrine, the chromophore is well protected and should result in a quantum yield that is independent of environment; thus,  $\xi$  should be a constant for proteins labeled with CFP and YFP. The physical basis of  $\xi$  is similar in concept to the factor  $G$  put forth by Gordon et al. (1998). Given the complexities in wavelength transmission in the microscope and the detector response,  $\xi$  was determined empirically, rather than calculated. When  $E_C$  is unknown, the apparent donor efficiency can be determined as the product of the true efficiency and the fraction of donor in complex,

$$E_D = E f_D = \left[ 1 - \frac{I_D}{(I_F - \alpha I_A - \beta I_D)(\xi/\gamma) + I_D} \right]. \quad (5)$$

### Acceptor–donor ratio ( $R$ )

Estimating total donor fluorescence in the absence of FRET allows determination of the absolute concentration ratio of acceptor  $[A_T]$  to donor  $[D_T]$ ,

$$R = \frac{[A_T]}{[D_T]} = \left( \frac{\xi}{\gamma^2} \right) \frac{\alpha I_A}{(I_F - \alpha I_A - \beta I_D)(\xi/\gamma) + I_D}. \quad (6)$$

FRET stoichiometry corrects for variable sample thickness, and therefore provides, at each pixel of the image, the relative concentrations of donor, acceptor, and complex. For bimolecular interactions,  $f_A$  and  $f_D$  will range from 0 to 1, indicating the fraction of acceptor- or donor-labeled molecules participating in a molecular complex.  $R = 1$  indicates that equal mole fractions of donors and acceptors are present in the image pixel,  $R > 1$  or  $< 1$  indicates an excess of either acceptor or donor, respectively. Measuring the complete stoichiometry,  $R$ ,  $f_A$ , and  $f_D$  (or  $R$ ,  $E_A$ , and  $E_D$ )

should be particularly useful for obtaining information about the numbers of interacting molecules and identifying the limiting binding partner of an interaction.

To examine the behavior of these equations relative to various conditions and to other methods (Xia and Liu, 2001; Miyawaki et al., 1997), we developed a static mathematical model based on high-affinity donor–acceptor interactions in which one species is limiting. Model conditions were defined in which all donor and acceptor were in complex, and FRET efficiency of those complexes varied (Fig. 2 *A*). Comparisons with current methods (Xia and Liu, 2001) indicated that, whereas  $E_A$  and  $E_D$  increased linearly with FRET efficiency, other methods were nonlinear, deviating dramatically as FRET efficiency approached 1.00 (Fig. 2 *A*). To compare the methods for their abilities to discriminate ratios of donor, acceptor, and complex, model conditions were defined such that FRET efficiency of the complex was fixed, and the ratios of complex to unlinked donor or acceptor were varied (Fig. 2, *B* and *C*).  $f_A$  varied linearly with the fraction of acceptor in complex (Fig. 2 *B*), but was independent of the fraction of donor in complex (Fig. 2 *C*). Conversely,  $f_D$  reflected the fraction of donor in complex (Fig. 2 *C*), but was unaffected by the presence of excess acceptor (Fig. 2 *B*). FRET stoichiometry was the only method that could distinguish between excess acceptor and excess donor, and could determine correctly the fractions of acceptor, donor, and complex.

The spectral variants of GFP are a good choice for FRET imaging because the chromophore is generally protected in the core of the protein. However, the chromophore of YFP is accessible to solvent and is sensitive to pH near neutrality (Elslinger et al., 1999) and to anions such as chloride (Jayaraman et al., 2000), making it a questionable acceptor for physiological conditions where pH or concentrations of ions can change. A recently discovered mutation of YFP (Q69M), called citrine, protects the chromophore and decreases the apparent  $pK_a$  to that observed for other fluorescent proteins (Griesbeck et al., 2001). We reasoned from work by Elslinger et al. (1999) that this mutation maintained the chromophore in the anionic form, which has a much greater absorbance than the neutral form of the chromophore; consequently citrine should have a longer Förster distance than YFP at pH near 7. Donor-based fluorescence lifetime measurements of FRET efficiency for purified molecules of either CFP covalently linked to YFP (CFP–YFP) or CFP covalently linked to citrine (CFP–Cit) confirmed this prediction (Fig. 3 *A*). The fluorescence lifetime of CFP in the purified CFP, CFP–YFP, and CFP–Cit sample at pH 7 were  $3.01 \pm 0.02$  ns,  $2.41 \pm 0.02$  ns, and  $1.81 \pm 0.01$  ns, respectively (average of three independent measurements  $\pm$  standard deviation). Because the proteins were identical except for the single point mutation at position 69 of YFP, the increased FRET efficiency of CFP–Cit at neutral pH indicated that the Förster distance for citrine and CFP was both pH-insensitive and nearly double that of YFP and CFP.

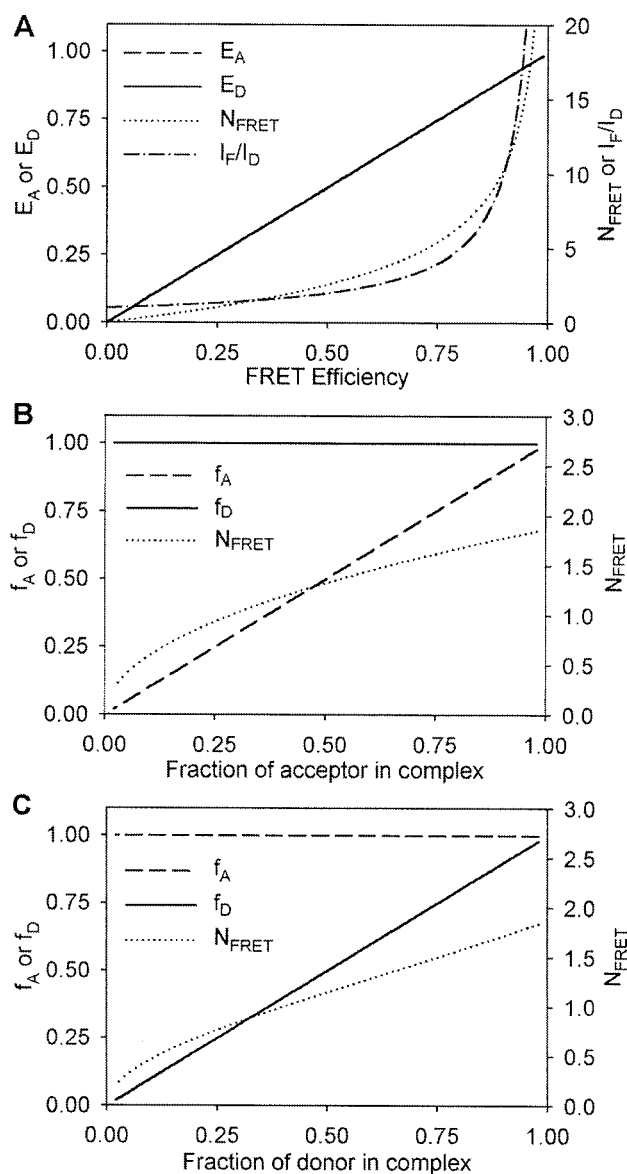


FIGURE 2 A mathematical model was generated in which all species and interactions depicted in Fig. 1 *C* were accounted for. (*A*) As FRET efficiency of donor–acceptor complexes increased,  $E_A$  and  $E_D$  remained linear, whereas other methods approached infinity. (*B*) For mixtures of acceptor plus complex,  $N_{FRET}$  was nonlinear, whereas the calculated  $f_A$  reproduced the fraction of acceptor in complex and  $f_D$  remained constant at a value of 1. (*C*) When the fraction of donor in complex was varied,  $N_{FRET}$  was nonlinear, whereas  $f_D$  reflected the fraction of donor in complex and  $f_A$  remained constant.

Therefore, for intracellular FRET studies, citrine was significantly better than YFP as a fluorescent acceptor.

To test the methods for calculation of  $f_A$ ,  $f_D$ , and  $R$ , microscopic measurements were collected from mixtures of purified CFP, citrine and CFP–Cit.  $E_C$  of CFP–Cit was determined from CFP fluorescence lifetime measurements to be 0.40 in solution (Fig. 3 *A*). As predicted, mixtures where the ratios of CFP–Cit to citrine were varied showed

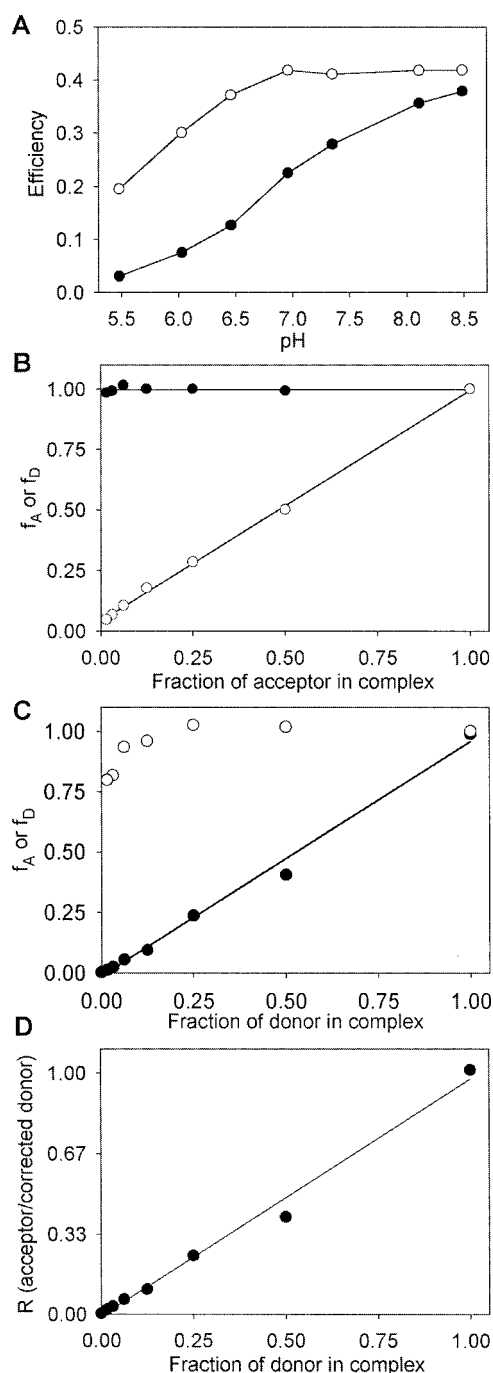


FIGURE 3 Verification of FRET stoichiometry by solution measurements of fluorescent proteins and enhanced energy transfer with citrine. (A) FRET efficiency was determined as a function of pH by donor fluorescence lifetime for both CFP alone and CFP-YFP or CFP-Cit. The pH-dependent YFP absorption greatly affected the FRET efficiency near neutral pH (closed circles) whereas citrine (open circles) was unaffected until lower pH (the data shown are averages of three independent measurements and the standard deviation is smaller than the data points). (B) 1  $\mu$ M CFP-Cit was serially diluted in 1  $\mu$ M citrine, then  $f_A$  (open circles) and  $f_D$  (closed circles) of the solutions were measured by microscopy. The x-axis is the pipetted fraction of donor or acceptor in complex. Because all donor (CFP) in the system was in complex,  $f_D$  was unaffected by the dilution, whereas  $f_A$  varied linearly with the fraction of acceptor in complex. (C) 1  $\mu$ M

the expected decrease in  $f_A$ , but no change in  $f_D$  (Fig. 3 B) reflecting the condition that variable amounts of citrine (acceptor) were not part of complexes, but all of the CFP (donor) was linked to citrine. Conversely, mixtures in which ratios of CFP-Cit to CFP were varied showed that  $f_D$  and  $f_A$  correctly measured the fraction of donor in complex (Fig. 3 C). The tailing off of  $f_A$  seen in Fig. 3 C is due to insufficient citrine left in the sample to produce an accurate  $I_A$  image. Thus,  $f_A$  and  $f_D$  accurately reported the fractions of acceptor, donor, and complex. Moreover,  $R$  was a good indicator of the ratio of acceptor to donor (Figs. 3 D). Taken together, the solution studies indicated that, if  $E_C$  is known, FRET stoichiometry could measure the ratios of donor, acceptor, and complex.

To determine whether fractions of donor or acceptor in complex could be measured in living cells, mixed stoichiometries of CFP, citrine, and CFP-Cit were created by transient transfection of J774 macrophages. Transfection with three combinations of plasmids—linked CFP-Cit plus CFP, linked CFP-Cit plus citrine, and citrine plus CFP (no-FRET control)—produced cells expressing different absolute amounts of CFP, citrine, and linked CFP-Cit, as well as different and unknown ratios of these fluorophores inside cells. Component images were collected from cells in the microscope, then  $f_A$ ,  $f_D$ , and  $R$  were calculated and displayed as digital images.  $E_C$  was independently measured by fluorescence lifetime of the donor on individual cells expressing CFP-Cit. In cells expressing CFP-Cit plus citrine (Fig. 4, A and B), the intensities of the component images varied widely, but the processed images representing  $f_A$ ,  $f_D$ , and  $R$  were uniform as expected for ubiquitously expressed soluble probes in the cytoplasm.  $f_A$  varied from cell to cell, indicating variation in the intracellular ratios of linked CFP-Cit and citrine due to variable protein expression. For example, the cell on the left of Fig. 4 B exhibited high  $R$  (Cit/CFP) and low  $f_A$ , indicating that it contained much more free citrine than linked CFP-Cit. In contrast,  $f_D$  remained uniformly high, indicating that all CFP in that cell was as linked CFP-Cit. In cells expressing linked CFP-Cit plus CFP,  $f_D$  was variable and  $f_A$  remained high (Fig. 4 C). In cells expressing CFP and citrine (no FRET) cellular ratios of CFP to citrine varied considerably with expression levels, but  $f_A$  and  $f_D$  were zero (Fig. 4 D).

In both the cell expression and solution studies mentioned above, image shading corrections were necessary to obtain uniform values of  $E_A$ ,  $E_D$ ,  $f_A$ ,  $f_D$ , and  $R$  across the image. This correction has not been applied in previous studies. For quantitation of FRET, it was necessary that the processed

CFP-Cit was diluted into 1  $\mu$ M CFP.  $f_D$  reflected the fraction of donor in complex, whereas  $f_A$  remained high, indicating that all citrine was in complex. (D) The data of (C) plotted to show the corrected ratio  $R$ .  $R$  accurately reflected the dilutions for both CFP-Cit plus CFP and CFP-Cit plus citrine (data not shown).



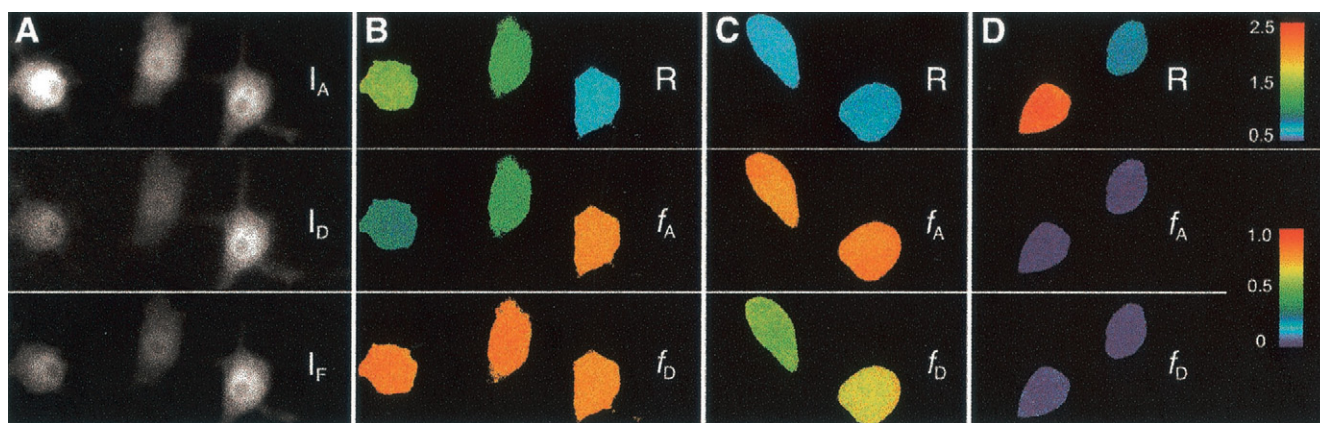


FIGURE 4 FRET stoichiometry imaging of J774 macrophages co-expressing CFP, citrine, or CFP-Cit. (A) Component images  $I_A$ ,  $I_D$ , and  $I_F$  for three cells expressing CFP-Cit plus citrine. Fluorescence intensities varied due to differing protein expression levels and to variable cell thickness. (B) Processed images from (A) showing  $R$  (citrine/CFP),  $f_A$ , and  $f_D$ .  $f_A$  was variable and inversely correlated with  $R$ , whereas  $f_D$  was constant at a value of 1.0, indicating that all donor was in complex. (C) Processed images of cells expressing CFP-Cit plus CFP indicated that  $f_A$  was constant at 1.0,  $f_D$  was variable and correlated with  $R$ . (D) Processed images of cells expressing CFP plus citrine;  $R$  differed but  $f_A$  and  $f_D$  remained uniformly at zero, indicating no FRET. Image calculations under all conditions gave uniform images, indicating that cell thickness was properly corrected for.

images give the correct values across the image for controls such as uniform solutions of CFP-Cit sandwiched between two coverglasses. Moreover, coregistration was also confirmed by looking for edge artifacts on cells imaged at various positions on the CCD camera.

The cumulative measurements from three combinations of expressed fluorophores reflected the relationships described by the models and the solution studies (Fig. 5). When CFP-Cit was coexpressed with Cit,  $f_A$  varied linearly with the ratio CFP/citrine ( $1/R$ ), whereas  $f_D$  remained uniformly high (indicating that all CFP in the cells was in complex; Fig. 5 A). The relationship was reversed, as anticipated, for cells coexpressing CFP-Cit and CFP:  $f_D$  varied linearly with the Cit/CFP ratio ( $R$ ) and  $f_A$  remained uniformly high (Fig. 5 B). Cells expressing unlinked citrine and CFP showed variable ratios of fluorophore expression (and variable fluorescence intensities, not shown), but never indicated the existence of complexes ( $f_D$  and  $f_A = 0$ ; Fig. 5 C). Thus, FRET stoichiometry could determine the complete stoichiometry of donor, acceptor, and donor-acceptor complexes in living cells. The methods were also quite sensitive, component images could be collected quickly (less than 200 ms/image) and repeatedly.

FRET stoichiometry was accurate and precise (Table 2). For all measurements in cells,  $f_A$ ,  $f_D$ , and  $R$  produced the expected value for each condition to within 1% and nearly all had standard deviations of  $<0.05$ , indicating that the precision was better than  $\pm 5\%$  of the measured molecules in complex (Table 2). Also, cells expressing CFP-Cit reproducibly gave an  $R$  value tightly distributed around 1 (Table 2). Importantly, in all of these measurements, the exposure time of 200 ms was held constant; only the neutral density filters on the microscope were used to vary the excitation from 1,  $1/4$ ,  $1/8$ , or  $1/32$  to obtain images within the

functional range of the CCD camera. Because the exposure time was not varied, and the neutral density adjustments were coarse, this means that some cells were imaged with varying contributions of noise (shot noise). FRET stoichiometry accurately determined the expected fractions of interacting molecules over a wide range of intensities; we expect the accuracy will improve as variable exposure times are used to collect images that have more optimal intensities. Cellular autofluorescence was the greatest limitation of FRET stoichiometry, for cells expressing low concentrations of fluorescent chimeras, yet autofluorescence had little effect on the measurements down to CFP intensities that were only twice that of the autofluorescence of neighboring untransfected cells (data not shown). Presumably, this is because the  $I_F - \beta I_D$  correction also removes much of the autofluorescence contributions from  $I_F$ .

## DISCUSSION

FRET stoichiometry applies three essential equations to measure interactions between fluorescent proteins inside living cells. After calibration of the microscope to determine  $\alpha$ ,  $\beta$ ,  $\gamma$ , and  $\xi$ , and determination of  $E_C$  for a particular bimolecular interaction, the quantities  $f_A$ ,  $f_D$ , and  $R$  for that interaction inside cells can be obtained from the fluorescence images  $I_A$ ,  $I_D$ , and  $I_F$ . Alternatively, if  $E_C$  is unknown or inappropriate to the chemistry being studied, then the quantities  $E_A$ ,  $E_D$ , and  $R$  can be measured. The quantities  $E_A$  and  $E_D$  are proportional to the fraction of acceptors or donors in complex, respectively, and can be used to measure changes in the fraction of molecules in complex.

The applicability of FRET stoichiometry was established in three ways. First, the equations were examined and



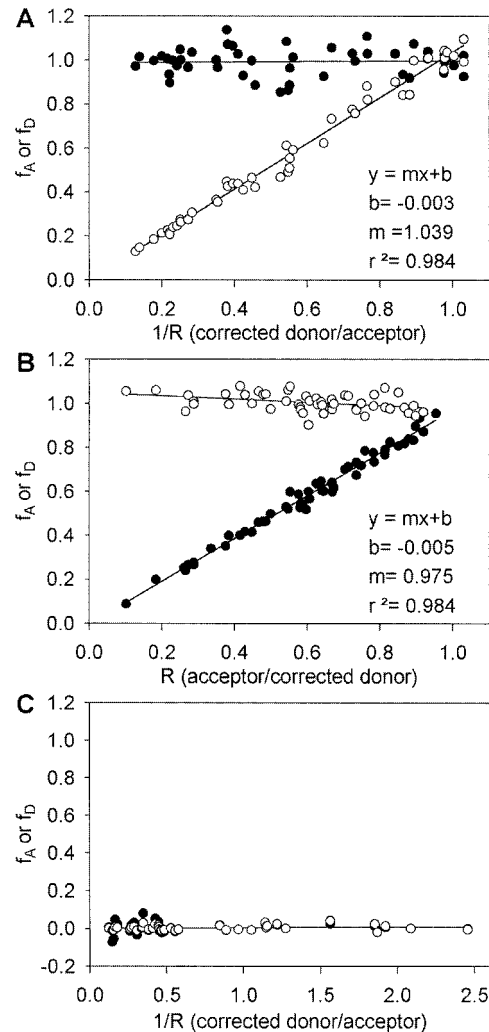


FIGURE 5 Cumulative measurements of  $R$ ,  $f_A$ , and  $f_D$  in J774 macrophages. (A) In cells expressing CFP–Cit plus citrine,  $f_D = 1$  (closed circles) and  $f_A$  (open circles) was linear with  $1/R$  (CFP/citrine) as indicated by the linear regression. (B) Cells expressing CFP–Cit plus CFP showed  $f_A = 1$  and  $f_D$  linear with  $R$  (citrine/CFP). (C) In cells expressing CFP plus citrine (no FRET),  $f_A$  and  $f_D$  were uniformly low, despite wide variation in citrine/CFP fluorescence ratios ( $R$ ). The data were well fit by linear regression analysis (lines,  $R^2 > 0.984$ ) and both  $f_A$  and  $f_D$  gave the expected 1:1 correlation with  $R$ .

compared to other methods using mathematical modeling. The modeling showed that the terms  $E_A$  and  $E_D$  scaled linearly with FRET efficiency and that the equations for  $f_A$

and  $f_D$  could accurately distinguish conditions of excess donor and excess acceptor, in contrast to other methods. Second, the equations were applied to microscopic images of mixtures of purified CFP, citrine, and linked CFP–Cit. The solution measurements showed that  $f_A$  and  $f_D$  correctly reported fractions of acceptor and donor, respectively, and the true ratios of total acceptor to total donor. Third, the equations were applied to cells expressing various mixtures of linked and unlinked fluorophores. Although the intracellular ratios of CFP, citrine, and linked CFP–Cit were unknown due to the variability of gene delivery and protein expression, the aggregate distributions of  $f_A$ ,  $f_D$ , and  $R$  in the measured populations of cells indicated that the measured stoichiometries were correct.

An essential feature of FRET stoichiometry is its application of characteristic FRET efficiency,  $E_C$ , to discriminate efficiency and fraction. The use of  $E_C$  to discriminate fractions of bound molecules is appropriate when the binding interaction gives rise to a reproducible efficiency. Multivalent interactions or FRET between molecules with multiple fluorophores attached to each molecule may add additional levels of complexity. Nonetheless, for bimolecular interactions, designating a characteristic value for the mean FRET efficiency of donor–acceptor complexes allowed stoichiometric measurement of reaction parameters: the ratios of bound and free donor and acceptor chimeras.  $E_C$  is most easily measured from linked constructs, such as CFP–Cit, in which all CFP and citrine are in complex (and both  $f_A$  and  $f_D$  equal one).  $E_C$  of linked CFP–Cit was measured using fluorescence lifetimes of free CFP and the CFP of linked CFP–Cit, then applied to determine  $\gamma$  and  $\xi$ . For stoichiometry of bimolecular interactions between unlinked fluorophores, we expect that donor–acceptor complexes will also have an  $E_C$ , which will have to be determined from equilibrium mixtures of free donor, free acceptor, and donor–acceptor complexes.  $E_C$  for unlinked fluorophores may be measurable in living cells by fluorescence lifetime-based methods (e.g., using curve fitting of CFP fluorescence decays). Alternatively,  $E_C$  may be obtainable from either solution or expression measurements of various ratios of donor and acceptor, identifying  $E_C$  as the maximum observed  $E_A$  and  $E_D$  in a range of mixtures. However, even if the characteristic efficiency is not known, FRET stoichiometry can still be used to measure  $E_A$  and  $E_D$ ; then, if  $E_C$  for

TABLE 2 FRET stoichiometry results for cell expression of combinations of linked and unlinked molecules

	CFP–Cit	Cit + CFP	CFP–Cit + CFP	CFP–Cit + Cit
Number of cells	55	40	55	47
$f_A \pm \text{SD}$	$1.00 \pm 0.018$	$0.004 \pm 0.014$	$1.005 \pm 0.047$	$\pm 0.039^\dagger$
$f_D \pm \text{SD}$	$1.00^* \pm 0.021$	$0.004 \pm 0.027$	$\pm 0.026^\dagger$	$0.992 \pm 0.047$
$R \pm \text{SD}$	$0.994 \pm 0.037$	—	—	—

\*These values were set to 1.00 for calculation of  $\gamma$  and  $\xi$ .  
†These values are the standard deviation of the residuals for the linear regressions given in Fig. 5.

that interaction is determined at a later point,  $f_A$  and  $f_D$  can be inferred from the original data.

For some intracellular chemistries, however, FRET efficiency will vary over a wide range of values, without a characteristic FRET efficiency for the interaction. For example, CFP and citrine chimeras that bind to membrane phospholipids could exhibit FRET as a function of lipid density in the bilayer (Kenworthy et al., 2000; Zacharias et al., 2002). In that case,  $E$  would be variable and fall over a wide range of values, and the terms  $f_A$  and  $f_D$  would not apply. Rather, the more general terms  $E_A$  and  $E_D$ , which incorporate both FRET efficiency and fractions of acceptor and donor in complex, would better describe the interactions. The utility of  $E_A$  was recognized in the earlier study of Erickson et al. (2001) whose term  $E_{\text{EFF}}$  was equivalent to  $E_A$ .

Some coefficients used to develop FRET stoichiometry were introduced in earlier studies.  $\alpha$  and  $\beta$  correct for non-FRET fluorescence of acceptor and donor in the FRET filter set, and are applied here just as they have been in many prior studies (Gordon et al., 1998; Xia and Liu, 2001; Erickson et al., 2001).  $\gamma$ , the ratio of extinction coefficients for acceptor and donor, excited at the donor's excitation, is an important descriptor of the donor-acceptor pair, and has been previously applied to measure FRET by stimulated emission, both in solutions (Lakowicz, 1999) and in the microscope (Erickson et al., 2001). However, unlike previous methods for obtaining  $\gamma$ , the methods for FRET stoichiometry obtained  $\gamma$  by back-calculation from measured values of  $E_C$ ,  $\alpha$ ,  $\beta$ ,  $I_A$ ,  $I_D$ , and  $I_F$  collected directly in the microscope using linked and unlinked CFP and citrine. The present study also develops and measures  $\xi$  for estimating the donor fluorescence lost due to FRET. Application of  $\xi$  was necessary for calculation of  $E_D$ ,  $f_D$ , and  $R$ , which are essential stoichiometric measurements of donor concentrations.  $\xi$  allows measurement of donor participation in FRET complexes, and eliminates the need for acceptor photobleaching to determine the fraction of energy lost from the donor. A similar term was used in the derivations of Gordon et al. (1998), although it was not applied or obtained in the microscope in that study.

The ability of FRET stoichiometry to measure  $R$ , the ratio of total acceptor to total donor, is valuable as a quantitative measure of relative concentrations even for molecules that do not exhibit FRET. Using a microscope calibrated for  $\alpha$ ,  $\beta$ ,  $\gamma$ , and  $\xi$ , the molar ratio of donor and acceptor fluorophores can be obtained inside a cell.  $R$  should facilitate studies of the relative local concentrations of CFP and citrine chimeras that do not associate with each other (i.e., no FRET) inside cells.

Fluorescent proteins are especially good fluorophores for live-cell FRET stoichiometry studies. A concern for calculation of  $E_D$  and  $f_D$  is that other mechanisms may be responsible for the loss of donor fluorescence for a molecular interaction. Because the chromophores of the fluores-

cent proteins are buried in the core of a protein, it is likely that dipolar energy transfer (rather than exchange mechanism or polarity change) is the dominant mechanism for the decrease in fluorescence of the donor (Tsien, 1998). Second, citrine (Griesbeck et al., 2001) removes the pH sensitivity of CFP/YFP energy transfer and is demonstrated here to have a much longer Förster distance than CFP/YFP. Both of these properties will improve FRET studies between fluorescent protein chimeras.

Complications of interpreting FRET data from fluorescent chimeras have been addressed by the development of linked biosensors (Miyawaki et al., 1997), in which CFP and YFP (or citrine) are linked together by protein domains that change donor-acceptor distances upon analyte binding or covalent modification (Miyawaki et al., 1999; Ting et al., 2001). Although linked biosensors reduce concerns about local concentrations of donor and acceptor ( $f_A$  and  $f_D$  equal one), they are difficult to create. Moreover, because they are not intrinsic elements of signaling pathways, they may miss many of the spatial dynamics obtainable using fluorescent chimeras of component molecules. Finally, linked biosensors may exhibit a smaller dynamic range than unlinked probes, because the linked biosensors typically exhibit some FRET even in their most open conformation (Miyawaki et al., 1997; Ting et al., 2001).

The ability to measure the binding stoichiometry of interacting fluorescent chimeras opens new areas of intracellular chemistry to quantitative study. Understanding of molecular systems in the cell will require quantitative comparisons of molecular events in space and time. FRET stoichiometry measures of the complete stoichiometry of fractions of acceptors in complex, donor in complex, and the ratio of donor molecules to acceptor molecules at each pixel in an image. Unlike previous biochemical and microscopic methods, FRET stoichiometry measures the location and stoichiometry of molecular interactions inside a living cell. Moreover, FRET stoichiometry can be generalized to the study of multimolecular interactions and membrane associations. It should therefore be especially useful for studies of the behaviors of molecules in their native pathways (Kraynov et al., 2000; Janetopoulos et al., 2001) and the binding dynamics of membrane localized proteins and microdomains (Zacharias et al., 2002). Unlike previous microscopic methods, which give measurements in arbitrary units that are specific to a given instrument, the measured quantities, fraction and efficiency, are physical parameters that are transferable not only from one molecular interaction to another, but also to other fluorescence technologies, such as confocal microscopy, flow cytometry, and high-throughput screening. Extension of FRET stoichiometry to higher throughput modalities should allow quantitative analysis of molecular interactions in populations of living cells.

## APPENDIX: THEORY OF FRET STOICHIOMETRY

### Existing measurements of FRET efficiency

In the fluorometer, FRET efficiency is reliably measured by three different approaches. The most direct approach is by the fluorescence lifetime of the donor molecule (Lakowicz, 1999). Efficiency is given by

$$E = \left[ 1 - \frac{\tau_{DA}}{\tau_D} \right], \quad (A1)$$

where  $\tau_D$  is the mean fluorescence lifetime of the donor,  $\tau_{DA}$  is the mean fluorescence lifetime of the donor in the presence of acceptor, where all donor is in complex with acceptor. This approach is powerful, in that the lifetime is an intrinsic property of fluorescence and does not depend on the concentration of donor molecules. A second approach, equally valid but dependent on concentration, uses the decrease in fluorescence emitted from the donor (Lakowicz, 1999), given by

$$E = \left[ 1 - \frac{F_{DA}(\lambda_D^{\text{ex}} \lambda_D^{\text{em}})}{F_D(\lambda_D^{\text{ex}} \lambda_D^{\text{em}})} \right] \left( \frac{1}{f_D} \right), \quad (A2)$$

where  $F_D(\lambda_D^{\text{ex}} \lambda_D^{\text{em}})$  is the donor fluorescence at a given concentration, and  $F_{DA}(\lambda_D^{\text{ex}} \lambda_D^{\text{em}})$  is the donor fluorescence, at the same concentration, in the presence of acceptor. For microscopy, this method has been approximated by measuring the fluorescence of the donor in the presence of acceptor,  $F_{DA}(\lambda_D^{\text{ex}} \lambda_D^{\text{em}})$ , then photobleaching the acceptor and measuring the increased donor fluorescence,  $F_D(\lambda_D^{\text{ex}} \lambda_D^{\text{em}})$  (Kenworthy et al., 2000). The third option, called sensitized emission, refers to the enhanced fluorescence observed from the acceptor due to energy transfer from the donor. This is obtained from the ratio of fluorescence from the acceptor in the presence,  $F_{AD}(\lambda_D^{\text{ex}} \lambda_A^{\text{em}})$ , and absence,  $F_A(\lambda_D^{\text{ex}} \lambda_A^{\text{em}})$ , of the donor (Lakowicz, 1999), exciting at the donor's excitation wavelength and detecting at the acceptor's emission wavelength,

$$E = \frac{\varepsilon_A(\lambda_D^{\text{ex}})}{\varepsilon_D(\lambda_D^{\text{ex}})} \left[ \frac{F_{AD}(\lambda_D^{\text{ex}} \lambda_A^{\text{em}})}{F_A(\lambda_D^{\text{ex}} \lambda_A^{\text{em}})} - 1 \right] \left( \frac{1}{f_A} \right), \quad (A3)$$

where  $\varepsilon_A(\lambda_D^{\text{ex}})$  and  $\varepsilon_D(\lambda_D^{\text{ex}})$  are the extinction coefficients, at the donor's excitation wavelength, of the acceptor and donor, respectively.  $f_A$  is the fractional labeling of the acceptor with donor, or the fraction of acceptor in complex with the donor. This method for calculation of FRET efficiency requires that the donor does not emit at the acceptor's emission wavelength.

### Imaging FRET efficiency by sensitized acceptor emission

A goal of live-cell imaging is to collect multiple fluorescence images as a cell responds to a stimulus. To optimize this measurement, exposure times must be minimized to reduce photobleaching, to maintain cell viability, and to collect data at frequent intervals. Others have used a fluorescence microscope that collects three images through excitation and emission bandpass filters (Gordon et al., 1998; Xia and Liu, 2001). These three images are donor excitation and donor emission,  $F(\lambda_D^{\text{ex}} \lambda_D^{\text{em}})$  or  $I_D$ , acceptor excitation and acceptor emission,  $F(\lambda_A^{\text{ex}} \lambda_A^{\text{em}})$  or  $I_A$ , and donor excitation and acceptor emission,  $F(\lambda_D^{\text{ex}} \lambda_A^{\text{em}})$  or  $I_F$ .  $I_D$  and  $I_A$  generally discriminate donor

and acceptor fluorescence, with negligible transmission of one fluorophore into the other's filter set. That is,

$$F_A(\lambda_D^{\text{ex}} \lambda_D^{\text{em}}) = 0, \quad (A4)$$

$$F_D(\lambda_A^{\text{ex}} \lambda_A^{\text{em}}) = 0. \quad (A5)$$

A second assumption is that the contributions of excitation light or fluorescence emission can be propagated from one filter combination to another by scalar factors.

To satisfy Eq. A3 in the microscope,  $F_{AD}(\lambda_D^{\text{ex}} \lambda_A^{\text{em}})$  and  $F_A(\lambda_D^{\text{ex}} \lambda_A^{\text{em}})$  must be obtained while correcting for donor fluorescence spectral contamination of the acceptor's emission. Second,  $F_A(\lambda_D^{\text{ex}} \lambda_A^{\text{em}})$ , the acceptor fluorescence in the absence of donor, must be determined even in the presence of donor. Provided the acceptor fluorescence is not modified by the physical interaction with the donor-labeled molecule and the donor is not excited at the acceptor's excitation (Eq. A5) then,

$$F_{AD}(\lambda_A^{\text{ex}} \lambda_A^{\text{em}}) = F_A(\lambda_A^{\text{ex}} \lambda_A^{\text{em}}). \quad (A6)$$

Given Eq. A6, and that the emission of the acceptor due to excitation at one wavelength is proportional to the emission at another excitation wavelength, the fluorescence of the acceptor alone can be determined in the presence of donor,

$$F_A(\lambda_D^{\text{ex}} \lambda_A^{\text{em}}) = \alpha F_{AD}(\lambda_A^{\text{ex}} \lambda_A^{\text{em}}) = \alpha I_A, \quad (A7)$$

where  $\alpha$  is measured in a sample containing only acceptor as

$$\alpha = \frac{F_A(\lambda_D^{\text{ex}} \lambda_A^{\text{em}})}{F_A(\lambda_A^{\text{ex}} \lambda_A^{\text{em}})}. \quad (A8)$$

In many cases, the fluorescence emission of the donor overlaps with the emission of the acceptor (as with CFP and citrine). Therefore, when both donor and acceptor are present, the signal collected in the acceptor emission with donor excitation,  $F(\lambda_D^{\text{ex}} \lambda_A^{\text{em}})$  or  $I_F$ , consists of fluorescence from both acceptor and donor,

$$F(\lambda_D^{\text{ex}} \lambda_A^{\text{em}}) = F_{AD}(\lambda_D^{\text{ex}} \lambda_A^{\text{em}}) + F_{DA}(\lambda_D^{\text{ex}} \lambda_A^{\text{em}}) = I_F. \quad (A9)$$

The donor fluorescence contribution to  $I_F$  can be determined from the donor image ( $I_D$ ) as

$$F_{DA}(\lambda_D^{\text{ex}} \lambda_A^{\text{em}}) = \beta F_{DA}(\lambda_D^{\text{ex}} \lambda_D^{\text{em}}) = \beta I_D, \quad (A10)$$

where the correction factor  $\beta$  comes from independent measurements of donor fluorescence in the FRET filter set relative to donor fluorescence in the donor filter set, absent acceptor,

$$\beta = \frac{F_D(\lambda_D^{\text{ex}} \lambda_A^{\text{em}})}{F_D(\lambda_D^{\text{ex}} \lambda_D^{\text{em}})}. \quad (A11)$$

Substituting Eqs. A7, A9, and A10 into the sensitized emission Eq. A3 gives

$$E = \frac{\varepsilon_A(\lambda_D^{\text{ex}})}{\varepsilon_D(\lambda_D^{\text{ex}})} \left[ \frac{F(\lambda_D^{\text{ex}} \lambda_A^{\text{em}}) - \beta F_{DA}(\lambda_D^{\text{ex}} \lambda_D^{\text{em}})}{\alpha F_A(\lambda_A^{\text{ex}} \lambda_A^{\text{em}})} - 1 \right] \left( \frac{1}{f_A} \right). \quad (A12)$$

These fluorescence contributions can be intensities or images collected through various combinations of excitation and emission filters. Thus, Eq. A12 can be expressed as

$$E = \gamma \left[ \frac{I_F - \beta I_D}{\alpha I_A} - 1 \right] \left( \frac{1}{f_A} \right). \quad (\text{A13})$$

$\gamma$  is the scalar relating the absorbance of the acceptor to absorbance of the donor at the donor's excitation (Lakowicz, 1999),

$$\gamma = \frac{\varepsilon_A(\lambda_D^{\text{ex}})}{\varepsilon_D(\lambda_D^{\text{ex}})}. \quad (\text{A14})$$

### Determination of $f_A$ by FRET stoichiometry

For a bimolecular binding event, the specific orientations and distances between the acceptor and donor fluorophores will be the same under a given set of conditions. That is, for a given bimolecular interaction, there is a characteristic efficiency of energy transfer  $E_C$ . Even if the bimolecular interaction results in a distance or orientation distribution between the donor and acceptor dipoles,  $E_C$  will still be specifically described by that binding event. Provided  $E_C$  can be determined, by fluorescence lifetime or other methods, then  $f_A$  can be measured as

$$f_A = \frac{[C]}{[A_T]} = \gamma \left[ \frac{I_F - \beta I_D}{\alpha I_A} - 1 \right] \left( \frac{1}{E_C} \right). \quad (\text{A15})$$

If not, then an apparent efficiency of transfer to the acceptor ( $E_A$ ) can still be measured. This efficiency is the product of the two unknowns,  $E$  and  $f_A$ , and is still quantitative in that changes in  $E_A$  reflect real changes in the number of acceptor-labeled molecules in complex

$$E_A = E f_A. \quad (\text{A16})$$

### FRET stoichiometry for efficiency and fraction of donor $f_D$

The sensitized emission fluorescence from the acceptor can also be used to determine the fluorescence of the donor in the unquenched state. Provided the only effect of the binding event on the acceptor and donor fluorescence is energy transfer, then conservation of energy dictates that the sensitized emission from the acceptor must be proportional to the loss of fluorescence from the donor. The fluorescence emitted by the acceptor can be thought of as the fluorescence due to direct excitation of the acceptor  $F_A(\lambda_D^{\text{ex}}\lambda_A^{\text{em}})$  plus the excitation of the acceptor due to energy transfer  $F_T(\lambda_D^{\text{ex}}\lambda_A^{\text{em}})$ . Incorporating this into Eq. A9 gives

$$\begin{aligned} F(\lambda_D^{\text{ex}}\lambda_A^{\text{em}}) &= F_{AD}(\lambda_D^{\text{ex}}\lambda_A^{\text{em}}) + F_{DA}(\lambda_D^{\text{ex}}\lambda_A^{\text{em}}) \\ &= F_A(\lambda_D^{\text{ex}}\lambda_A^{\text{em}}) + F_T(\lambda_D^{\text{ex}}\lambda_A^{\text{em}}) + F_{DA}(\lambda_D^{\text{ex}}\lambda_A^{\text{em}}). \end{aligned} \quad (\text{A17})$$

Combining A17 with A7 and A10, the fluorescence from the acceptor due to energy transfer is

$$F_T(\lambda_D^{\text{ex}}\lambda_A^{\text{em}}) = F(\lambda_D^{\text{ex}}\lambda_A^{\text{em}}) - \alpha F_{AD}(\lambda_A^{\text{ex}}\lambda_A^{\text{em}}) - \beta F_{DA}(\lambda_D^{\text{ex}}\lambda_D^{\text{em}}). \quad (\text{A18})$$

The total quantity of fluorescence emitted from the unquenched donor can be obtained as

$$F_D(\lambda_D^{\text{ex}}\lambda_D^{\text{em}}) = F_T(\lambda_D^{\text{ex}}\lambda_A^{\text{em}}) \frac{\xi}{\gamma} + F_{DA}(\lambda_D^{\text{ex}}\lambda_D^{\text{em}}), \quad (\text{A19})$$

where  $\xi$  corrects for the quantum yield of the acceptor and the quantity of photons that are collected in the acceptor emission relative to those that would have been collected in the donor emission if there were no energy transfer. Combining Eq. A19 with the definition of efficiency for energy transfer from the donor (Eq. A2),  $E$  from the donor fluorescence is obtained,

$$E = \left[ 1 - \frac{F_{DA}(\lambda_D^{\text{ex}}\lambda_D^{\text{em}})}{F_T(\lambda_D^{\text{ex}}\lambda_A^{\text{em}})(\xi/\gamma) + F_{DA}(\lambda_D^{\text{ex}}\lambda_D^{\text{em}})} \right] \left( \frac{1}{f_D} \right). \quad (\text{A20})$$

Written in terms of the three acquired images, this becomes

$$E = \left[ 1 - \frac{I_D}{(I_F - \alpha I_A - \beta I_D)(\xi/\gamma) + I_D} \right] \left( \frac{1}{f_D} \right). \quad (\text{A21})$$

If the characteristic efficiency,  $E_C$ , is known, then  $f_D$  can be determined as

$$f_D = \frac{[C]}{[D_T]} = \left[ 1 - \frac{I_D}{(I_F - \alpha I_A - \beta I_D)(\xi/\gamma) + I_D} \right] \left( \frac{1}{E_C} \right). \quad (\text{A22})$$

If  $E_C$  is unknown, an apparent efficiency ( $E_D$ ) can be determined as

$$E_D = E f_D. \quad (\text{A23})$$

### Obtaining $R$

The absolute ratio of acceptor molecules to donor molecules can be determined as the ratio of acceptor fluorescence (independent of FRET) to that of the corrected donor fluorescence by calculating the ratio of Eqs. A22 to A15,

$$R = \frac{[A_T]}{[D_T]} = \left( \frac{\xi}{\gamma^2} \right) \frac{\alpha I_A}{(I_F - \alpha I_A - \beta I_D)(\xi/\gamma) + I_D}. \quad (\text{A24})$$

This equation is the indicator of the mole fraction of total acceptors to total donors per pixel.

We thank D. Axelrod, K. Hahn, D. Kirschner, M. Swanson, and N. Thiec for suggestions, and S. Schreiber for assistance.

This work was supported in part by National Institutes of Health grant AI35950 to J.S. A.H. was supported by National Institutes of Health Cellular Biotechnology Training Program.

### REFERENCES

- Elslinger, M. A., R. M. Wachter, G. T. Hanson, K. Kallio, and S. J. Remington. 1999. Structural and spectral response of green fluorescent protein variants to changes in pH. *Biochemistry*. 38:5296–5301.
- Erickson, M. G., B. A. Alseikhan, B. Z. Peterson, and D. T. Yue. 2001. Preassociation of calmodulin with voltage-gated Ca(2+) channels revealed by FRET in single living cells. *Neuron*. 31:973–985.
- Gordon, G. W., G. Berry, X. H. Liang, B. Levine, and B. Herman. 1998. Quantitative fluorescence resonance energy transfer measurements using fluorescence microscopy. *Biophys. J.* 74:2702–2713.



- Griesbeck, O., G. S. Baird, R. E. Campbell, D. A. Zacharias, and R. Y. Tsien. 2001. Reducing the environmental sensitivity of yellow fluorescent protein. Mechanism and applications. *J. Biol. Chem.* 276: 29188–29194.
- Janetopoulos, C., T. Jin, and P. Devreotes. 2001. Receptor-mediated activation of heterotrimeric G-proteins in living cells. *Science*. 291: 2408–2411.
- Jayaraman, S., P. Haggie, R. M. Wachter, S. J. Remington, and A. S. Verkman. 2000. Mechanism and cellular applications of a green fluorescent protein-based halide sensor. *J. Biol. Chem.* 275:6047–6050.
- Kenworthy, A. K., N. Petranova, and M. Edidin. 2000. High-resolution FRET microscopy of cholera toxin B-subunit and GPI-anchored proteins in cell plasma membranes. *Mol. Biol. Cell*. 11:1645–1655.
- Kraynov, V. S., C. Chamberlain, G. M. Bokoch, M. A. Schwartz, S. Slabaugh, and K. M. Hahn. 2000. Localized Rac activation dynamics visualized in living cells. *Science*. 290:333–337.
- Lakowicz, J. R. 1999. Principles of Fluorescence Spectroscopy. Kluwer Academic/Plenum, New York.
- Miyawaki, A., O. Griesbeck, R. Heim, and R. Y. Tsien. 1999. Dynamic and quantitative  $\text{Ca}^{2+}$  measurements using improved cameleons. *Proc. Natl. Acad. Sci. U.S.A.* 96:2135–2140.
- Miyawaki, A., J. Llopis, R. Heim, J. M. McCaffery, J. A. Adams, M. Ikura, and R. Y. Tsien. 1997. Fluorescent indicators for  $\text{Ca}^{2+}$  based on green fluorescent proteins and calmodulin. *Nature*. 388:882–887.
- Sourjik, V., and H. C. Berg. 2002. Receptor sensitivity in bacterial chemotaxis. *Proc. Natl. Acad. Sci. U.S.A.* 99:123–127.
- Ting, A. Y., K. H. Kain, R. L. Klemke, and R. Y. Tsien. 2001. Genetically encoded fluorescent reporters of protein tyrosine kinase activities in living cells. *Proc. Natl. Acad. Sci. U.S.A.* 98:15003–15008.
- Tron, L., J. Szollosi, S. Damjanovich, S. H. Helliwell, D. J. Arndt-Jovin, and T. M. Jovin. 1984. Flow cytometric measurement of fluorescence resonance energy transfer on cell surfaces. Quantitative evaluation of the transfer efficiency on a cell-by-cell basis. *Biophys. J.* 45:939–946.
- Tsien, R. Y. 1998. The green fluorescent protein. *Annu. Rev. Biochem.* 67:509–544.
- Xia, Z., and Y. Liu. 2001. Reliable and global measurement of fluorescence resonance energy transfer using fluorescence microscopes. *Biophys. J.* 81:2395–2402.
- Youvan, D. C., C. M. Silva, E. J. Bylina, W. J. Coleman, M. R. Dilworth, and M. M. Yang. 1997. Calibration of fluorescence resonance energy transfer in microscopy using genetically engineered GFP derivatives on nickel chelating beads. *Biotechnology*. 3:1–18.
- Zacharias, D. A., J. D. Violin, A. C. Newton, and R. Y. Tsien. 2002. Partitioning of lipid-modified monomeric GFPs into membrane microdomains of live cells. *Science*. 296:913–916.